DRIFT WAVES IN A TWO ION SPECIES PLASMA

Masaaki Watanabe
Department of Electrical Engineering
and Computer Sciences
Electronics Research Laboratory
University of California, Berkeley, California
94720

The problems associated with impurities in possible fusion reactors have been known for years. They are primarily related with the energy loss by the enhanced radiation due to impurity ions. It is also known that the existence of impurity ions destabilizes a new type of drift instabilities due to impurity ions.[1] Although some characteristics of impurity ion drift instabilities have been investigated by B. Coppi et. al.[1], the detailed characteristics have not been studied. In this note we present numerical solutions of the dispersion relation of impurity ion drift instabilities, analysis of stabilizing effect of the ordinary drift wave by the presence of impurity ions, and an experimental study of the drift waves in two ion species plasma in Q-device.

The equilibrium studied consists of a light ion species plasma column surrounded by a heavy ion species (refers to impurity ions). For the analysis, these two plasma columns are approximated by a slab model where the d.c. magnetic field and the density gradient are in z and x direction, respectively. Assuming a Maxwellian velocity distribution for each species, the linearized Vlasov equation is solved in the electrostatic approximation for a perturbation of the form exp $i(\omega t + k_y y + k_z z)$. The perturbed density $\tilde{n}_j$ for j-th species plasma can be expressed in terms of the perturbed potential $\tilde{\phi}$,

$$\frac{\tilde{n}_j}{n_j} = -\frac{q_j e\tilde{\phi}}{T_j} \left\{ 1 - \left(1+W_j\left(\frac{\omega}{k_z V_{T_j}}\right)\right) Q_j \frac{\omega+\omega_j}{\omega} \right\} \tag{1}$$

where n, T, q are the density, temperature, charge number and sign, respectively, $V_{T_j} = \sqrt{\frac{2T_j}{m_j}}$ is the thermal velocity, $\omega_j = \frac{k_y T_j}{q_j e B_o} \frac{1}{n_j} \frac{dn_j}{dx}$ is the diamagnetic drift angular frequency and $Q_j = e^{-b_j} I_o(b_j)$ is the finite Larmor radius correction term with $b_j = \frac{k_y^2 a_j^2}{2}$, a_j being the Larmor radius of j-th species. The W-function can be expressed in terms of a Z-function,[2]

$$W_j(\zeta) = -1 + \zeta Z(\zeta) \tag{2}$$

and the dispersion relation is obtained by substituting equation (1) into the quasi-neutrality condition $\sum_j q_j \tilde{n}_j = 0$[1].

Numerical solution of the dispersion relation has been obtained for the following parameters; $q_L = 1$, $q_H = 5$, $T_e/T_L = 2$, $T_e/T_H = 10$,

$m_H/m_L = 50$, $r_{pL}/r_{pH} = -1$, $0 \leq n_H/n_L \leq 1.0$, $10^{-4} \leq -r_{pL}/\lambda_Z \leq 10^{-1}$,

$\left(\frac{1}{r_{pj}} = \frac{1}{n_j}\frac{dn_j}{dx}\right)$, having a Tokamak device in mind. In the review paper on the Tokamak device by Artismovich,[3] the experimental parameters achieved are $T_e \simeq 1.5$ keV, $T_i \simeq 500$ eV, $n = 5\times10^{13}$, $cm.^{-3}$ The charge number of impurity ions was chosen to approximate C^{4+}, N^{7+}, as possible impurities. Since impurity arises near the wall, the temperature of the heavy ion species was assumed lower than that of light ion species so that the parameter $T_e/T_H = 10$ was chosen. No significant change of the characteristic of the drift waves for $1 \lesssim T_e/T_H \lesssim 10$ was obtained in the numerical calculation.

In Fig. 1(a) are shown the frequency characteristics for the impurity ion drift wave where the phase velocity V_p along the magnetic field satisfies the inequality $V_{Te} >> V_{TL} > V_p > V_{TH}$, i.e.,

$V_{Te}/V_{TL} >> 1 > \frac{\omega}{k_z V_{TL}} > 0.06$. In this phase velocity regime the light

ion species with $V \simeq V_p$ is strongly resonant with the wave leading to wave growth while the heavy ion species adds some Landau damping. The wave in Fig. 1(a) is unstable for weak magnetic field, i.e., large values of $k_y a_L$ (since the quantity $k_y a_L$ is proportional to $\frac{1}{B}$) and stabilized

at strong magnetic field. As the quantity $\frac{\omega_L}{k_z V_{TL}} = \frac{1}{4\pi} \frac{\lambda_Z}{r_{pL}} k_y a_L \simeq 8.0\, k_y a_L$

(λ_z is the wavelength along the magnetic field) becomes larger than

$\frac{\omega}{k_z V_{TL}}$ (see Fig. 1(c)), i.e., $\omega < \omega_L$ for weak magnetic field, the wave is destabilized in a similar manner to the ordinary drift wave[4] where the electron and ion roles are played by light and heavy ion species. As the density gradient becomes more steep as in Fig. 1(b), the wave becomes more unstable. The wave, however, becomes a damped light ion acoustic wave as the density of heavy ion species increases as shown in Fig. 1(d). We did not find any unstable wave in the fluid regime classified as

$V_{T_e} >> V_p > V_{T_L} > V_{T_H}$ which correspond to the wave in Fig. 1(d). The wave in fluid regime was considered to be possibly unstable in reference 1.

Plotted in Fig. 2 is the stability diagram of drift waves in a two ion species plasma with opposing density gradients. The instability condition of the impurity ion drift wave in reference (1) has been obtained assuming $\omega \simeq - \omega_L$, $n_H << n_L$ so that

$$\frac{r_{pH}}{r_{pL}} + \frac{q_H n_H}{\frac{T_L}{T_e} n_e + n_L} < 0 \tag{3}$$

Since the total plasma density gradient becomes a zero at $\frac{n_H}{n_L} = 0.2$, the ordinary drift wave becomes stable as seen in Fig. 2, while the impurity ion drift wave is not stabilized since a density gradient of two ion species is still present.

Since in the slab model the density gradient lengths of two ion species plasma are opposite and equal, i.e., $r_{pL} = - r_{pH}$, the plasma is symmetric with respect to the ion species. Another instability regime should appear then as the heavy ion species becomes dominant for large values of $\frac{n_H}{n_L}$. The large $\frac{n_H}{n_L}$ was not considered to be of sufficient interest to investigate numerically, however, in the following analysis a band of stability is shown to occur between the unstable regimes.

Considering the ordinary drift wave regime $V_{T_e} > V_p >> V_{T_L} > V_{T_H}$

the W-function is approximately $W_e \simeq -1 + i\sqrt{\pi}\,\dfrac{\omega}{k_z V_{T_e}}$, $W_L \simeq \dfrac{k_z^{\,2}\, V_{TL}^2}{2\omega^2}$,

$$W_H \simeq \frac{k_z^{\,2}\, V_{TH}^2}{2\omega^2} \quad .$$

In the region of interest $\omega = \omega_R + i\,\omega_I$ with $\omega_R >> \omega_I$ and neglecting $\left(\dfrac{k_z V_{T_L}}{\omega}\right)^2, \left(\dfrac{k_z V_{T_H}}{\omega}\right)^2 << 1$, the dispersion relation becomes

$$\omega_R = \frac{\alpha_L Q_L \omega_L + \alpha_H Q_H \omega_H}{1 + \alpha_L(1-Q_L) + \alpha_H(1-Q_H)} \tag{4a}$$

$$\omega_I = \sqrt{\pi}\,\frac{\omega_R}{k_z V_{T_e}}\;\frac{\omega_R + \omega_e}{1 + \alpha_L(1-Q_L) + \alpha_H\,(1 - Q_H)} \tag{4b}$$

Making use of the relations $\omega_L = -\dfrac{q_H T_L}{q_L T_H}\,\omega_H$, $-\omega_e = \alpha_L\omega_L + \alpha_H\omega_H$, $Q_L \simeq 1-b_L$, $Q_H \simeq 1-b_H$, we obtain

$$\begin{aligned}\omega_I = -\frac{2\sqrt{\pi}}{k_z V_{Te}}\;&\frac{(1-b_H)\, b_H\, \omega_H^{\,2}}{(1+\alpha_L b_L + \alpha_H b_H)^3}\left(\frac{T_e}{T_H}\,q_H^{\,2}\right)^3\left(1 + \frac{1-b_L}{1-b_H}\right)\left(1 - \frac{m_L}{m_H}\,\frac{q_H}{q_L}\right)\\ &\cdot\left(\frac{n_H}{n_e} - \frac{1}{q_H}\,\frac{1-b_L}{2-b_L-b_H}\right)\left\{\left(\frac{n_H}{n_e}\right)^2 + \frac{1}{2}\,\frac{T_H}{T_e q_H^{\,2}}\;\frac{1 - \dfrac{T_e}{T_H}\,q_H + \dfrac{b_L}{b_H}\left(1 + 3\,\dfrac{T_e}{T_L}\,q_L\right)}{1 - \dfrac{m_L}{m_H}\,\dfrac{q_H}{q_L}}\;\frac{n_H}{n_e}\right.\\ &\left. - \frac{1}{2}\,\frac{m_L}{m_H}\,\frac{T_L}{q_H q_L^{\,2} T_e}\;\frac{1 + \dfrac{T_e}{T_L}\,q_L}{1 - \dfrac{m_L}{m_H}\,\dfrac{q_H}{q_L}}\right\}\end{aligned} \tag{5}$$

For the parameters used in Fig. 2, the stability band $\omega_I > 0$ appears in the narrow range $0.200 < \frac{n_H}{n_L} < 0.204$.

The above numerical calculations and analysis have been considered for Q-device parameters ($q_L = q_H = 1$, $T_e = T_L = T_H$). From equation (5), the ordinary drift wave is stabilized for $\frac{\sqrt{b_L}}{\sqrt{b_L} + \sqrt{b_H}} < \frac{n_H}{n_e} < 0.5$ as shown in Fig. 3. An expansion of the W-function to obtain a simplified dispersion relation for the impurity ion drift wave is in question since the maximum ratio of the two ion species thermal velocities in Q-device is at most 4.5 for a Li-Cs plasma. Since the velocity spread between two ion species may not be large enough to destabilize the wave, numerical calculations of the dispersion relation were done. No unstable waves in the phase velocity range of the impurity ion drift waves were found. It was not possible, however, to rule out categorically the existence of unstable waves with our numerical calculation method.

An experiment was performed in the BA-II (Berkeley Alkali-II) Q-device described elsewhere.[5] In addition to the usual plasma, a surrounding plasma having a heavy ion species was provided with a neutral beam from an annular nozzle. Investigations were conducted with a Lithium (or Potassium) plasma column surrounded by a Cesium (or Potassium) plasma.

Measurements of the ion saturation current across the plasma column are shown in Fig. 4(a), (b), (c). Fig. 4(d) shows a density profile of Fig. 4(c) corrected for the difference of thermal velocity of two ion species. Fig. 4(a) and (b) show the outer Potassium and central Lithium plasma, respectively. The separate density profiles were assumed to be unchanged when both species were present together as in Fig. 4(c) or (d) since only collisionless conditions were investigated. The oscillations shown in Fig. 4(b) for the central column only were observed at the indicated radial position and identified as ordinary drift waves[5] by observing that the waves propagate in the electron diamagnetic drift direction. No drift wave oscillations were observed with the outer plasma only although the slab model analysis predicts unstable ordinary drift waves. The observed stability of the annular plasma is possibly due to a stabilizing centrifugal force due the plasma rotation associated with radial electric field.

In the case shown in Fig. 4(c) or (d), the oscillations shown in Fig. 4(c) were found to propagate in the heavy ion diamagnetic drift direction. Since propagation is not in the direction of either the electron or light ion diamagnetic drift, it is concluded that neither the impurity ion drift waves or the ordinary drift wave is present. The experiment was performed both for single and double ended operation.

ACKNOWLEDGMENT

The author would like to express thanks to Dr. C. W. Hartman and Professor C. K. Birdsall for their useful advice and continuous support during this work.

This work is supported by AEC Contract AT(04-3)-34 Project 128.

REFERENCES

1. B. Coppi, H. P. Furth, M. N. Rosenbluth and R. Z. Sagdeev, Phys. Rev. Lett. 17 377 (1966)

2. B. D. Fried and S. D. Conte, "The Plasma Dispersion Function", Academic Press, Inc., New York, 1961

3. L. A. Artsimovich, Nuclear Fusion 12 215 (1972)

4. D. Meade, Phys. Fluids 12 447 (1969)

5. M. Watanabe and C. W. Hartman, (to be published).

FIGURE CAPTIONS

Fig. 1 Characteristics of the impurity ion drift wave obtained from numerical solution of the dispersion relation[1] for parameters $q_L = 1$, $q_H = 5$, $T_e/T_L = 2$, $T_e/T_H = 10$, $r_{pL}/r_{pH} = -1$, $m_H/m_L = 50$.

(a) $\dfrac{\omega}{k_z V_{TL}}$ v.s. $k_y a_L$ for $r_{pL}/\lambda_z = -10^{-2}$, $\dfrac{n_H}{n_L} = 0.1$.

(b) $\dfrac{\omega}{k_z V_{TL}}$ v.s. $k_y a_L$ for $r_{pL}/\lambda_z = -10^{-3}$, $\dfrac{n_H}{n_L} = 0.1$.

(c) $\dfrac{\omega}{k_z V_{TL}}$ v.s. $-\dfrac{r_{pL}}{\lambda_z}$ for $k_y a_L = 0.01$, $\dfrac{n_H}{n_L} = 0.1$.

(d) $R_e \dfrac{\omega}{k_z V_{TL}}$ v.s. $k_y a_L$ for $\dfrac{n_H}{n_L} = 0.5$.

Fig. 2 Stability diagram of the drift waves in a two ion species plasma obtained from numerical solutions of the dispersion relation[1] for parameters; $q_L = 1$, $q_H = 5$, $T_e/T_L = 2$, $T_e/T_H = 10$, $m_H/m_L = 50$, $r_{pL}/r_{pH} = -1$, $k_y a_L = 0.01$.

///// : unstable region for the impurity ion drift wave

\\\\\ : unstable region for the ordinary drift wave.

Fig. 3 ω_R , ω_I v. s. $\alpha_H = \dfrac{h_H}{n_e}$ for Q-device parameters ($q_L = q_H = 1$, $T_e = T_L = T_H$)

FIGURE CAPTIONS

Fig. 1 Characteristics of the impurity ion drift wave obtained from numerical solution of the dispersion relation[1] for parameters $q_L = 1$, $q_H = 5$, $T_e/T_L = 2$, $T_e/T_H = 10$, $r_{pL}/r_{pH} = -1$, $m_H/m_L = 50$.

(a) $\frac{\omega}{k_z V_{TL}}$ v.s. $k_y a_L$ for $r_{pL}/\lambda_z = -10^{-2}$, $\frac{n_H}{n_L} = 0.1$.

(b) $\frac{\omega}{k_z V_{TL}}$ v.s. $k_y a_L$ for $r_{pL}/\lambda_z = -10^{-3}$, $\frac{n_H}{n_L} = 0.1$.

(c) $\frac{\omega}{k_z V_{TL}}$ v.s. $-\frac{r_{pL}}{\lambda_z}$ for $k_y a_L = 0.01$, $\frac{n_H}{n_L} = 0.1$.

(d) $R_e \frac{\omega}{k_z V_{TL}}$ v.s. $k_y a_L$ for $\frac{n_H}{n_L} = 0.5$.

Fig. 2 Stability diagram of the drift waves in a two ion species plasma obtained from numerical solutions of the dispersion relation[1] for parameters; $q_L = 1$, $q_H = 5$, $T_e/T_L = 2$, $T_e/T_H = 10$, $m_H/m_L = 50$, $r_{pL}/r_{pH} = -1$, $k_y a_L = 0.01$.

///// : unstable region for the impurity ion drift wave

\\\\\ : unstable region for the ordinary drift wave.

Fig. 3 ω_R , ω_I v. s. $\alpha_H = \frac{h_H}{n_e}$ for Q-device parameters ($q_L = q_H = 1$, $T_e = T_L = T_H$)

Fig. 4 Measured ion saturation current for a two ion species plasma in single-ended operation.

(a) Outer Potassium plasma column only. Peak density $n_o = 4x10^9$ cm^{-3}. No oscillation in the valley of plasma was observed.

(b) Central Lithium plasma column only. Peak density $n_o = 1.5 \times 10^9$ cm^{-3} . Oscillations are measured at the marked radial position.

(c) Both of outer Potassium and central Lithium plasma column Oscillations are measured at the valley of two ion plasma.

(d) Total plasma density profile corrected for the difference of ion thermal velocity for the measurement of (c).

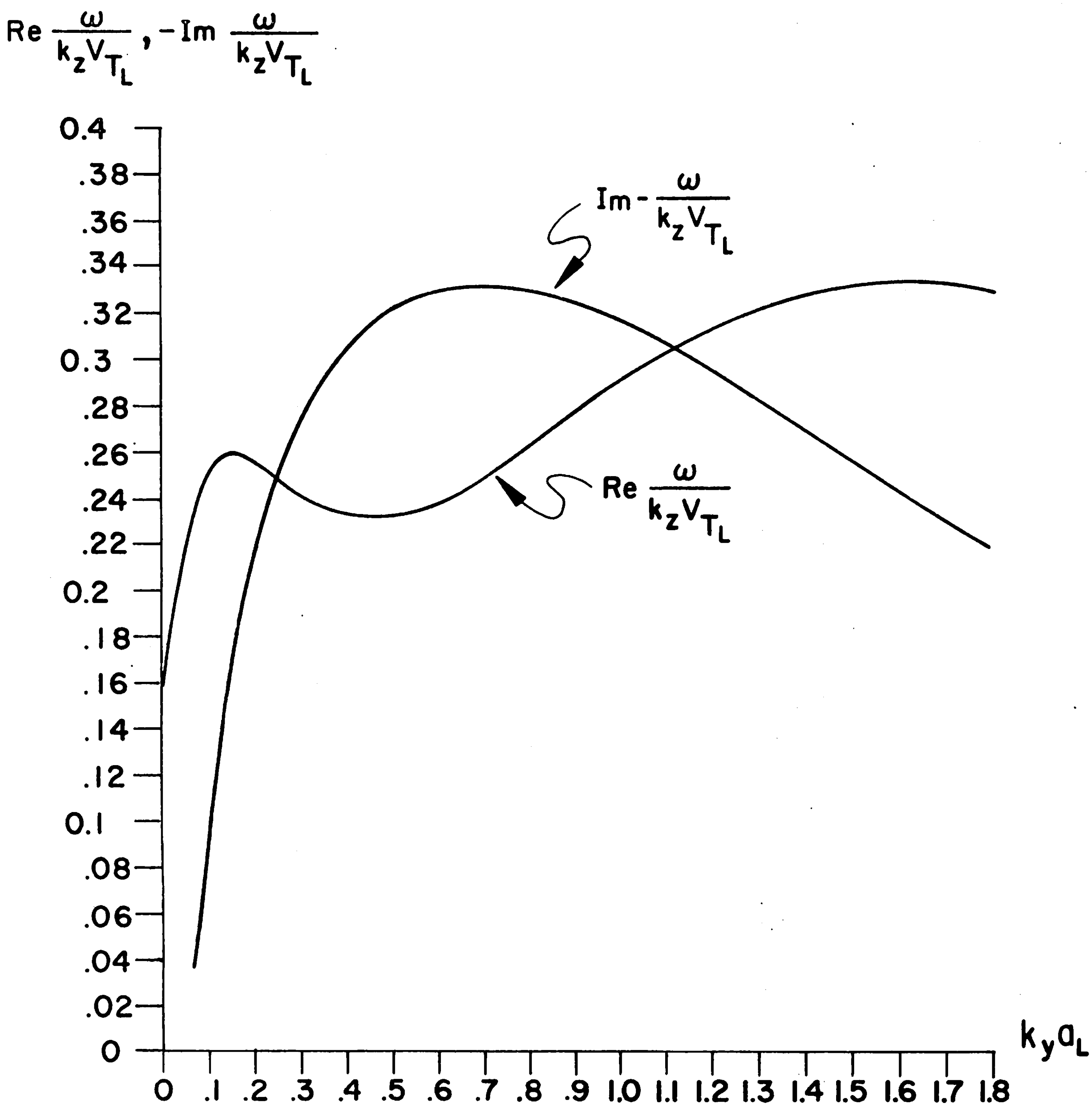

$\mathrm{Re}\,\frac{\omega}{k_z V_{T_L}}, -\mathrm{Im}\,\frac{\omega}{k_z V_{T_L}}$
0.4
.38
.36
.34
.32
0.3
.28
.26
.24
.22
0.2
.18
.16
.14
.12
0.1
.08
.06
.04
.02
0
$\mathrm{Im} - \frac{\omega}{k_z V_{T_L}}$
$\mathrm{Re}\,\frac{\omega}{k_z V_{T_L}}$
0
.1
.2
.3
.4
.5
.6
.7
.8
.9
1.0
1.1
1.2
1.3
1.4
1.5
1.6
1.7
1.8
$k_y a_L$

Fig. 1a

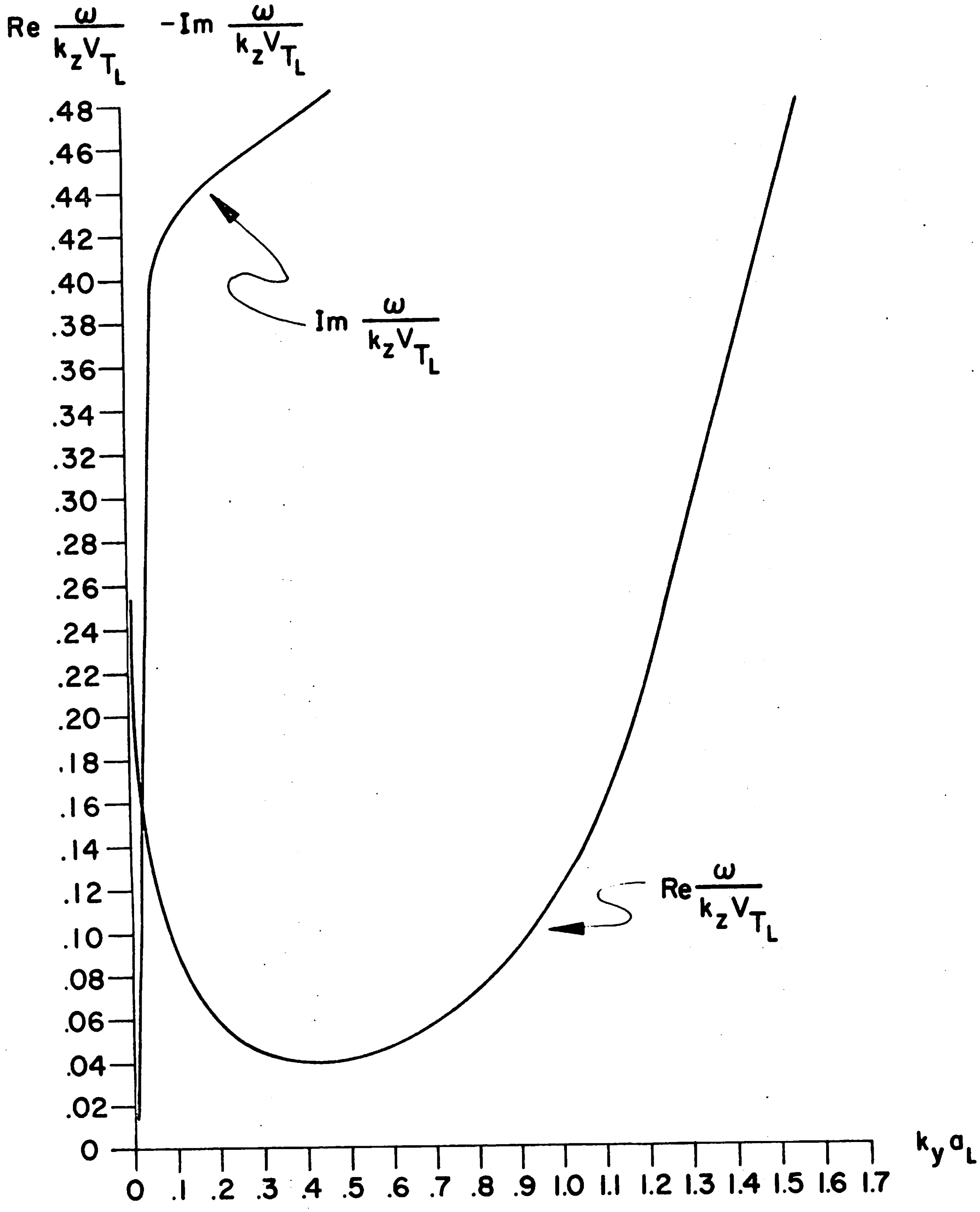

$\mathrm{Re}\,\frac{\omega}{k_z V_{T_L}}$ $-\mathrm{Im}\,\frac{\omega}{k_z V_{T_L}}$
.48
.46
.44
.42
.40
.38
.36
.34
.32
.30
.28
.26
.24
.22
.20
.18
.16
.14
.12
.10
.08
.06
.04
.02
0
$\mathrm{Im}\,\frac{\omega}{k_z V_{T_L}}$
$\mathrm{Re}\,\frac{\omega}{k_z V_{T_L}}$
0 .1 .2 .3 .4 .5 .6 .7 .8 .9 1.0 1.1 1.2 1.3 1.4 1.5 1.6 1.7
$k_y a_L$

Fig. 1b

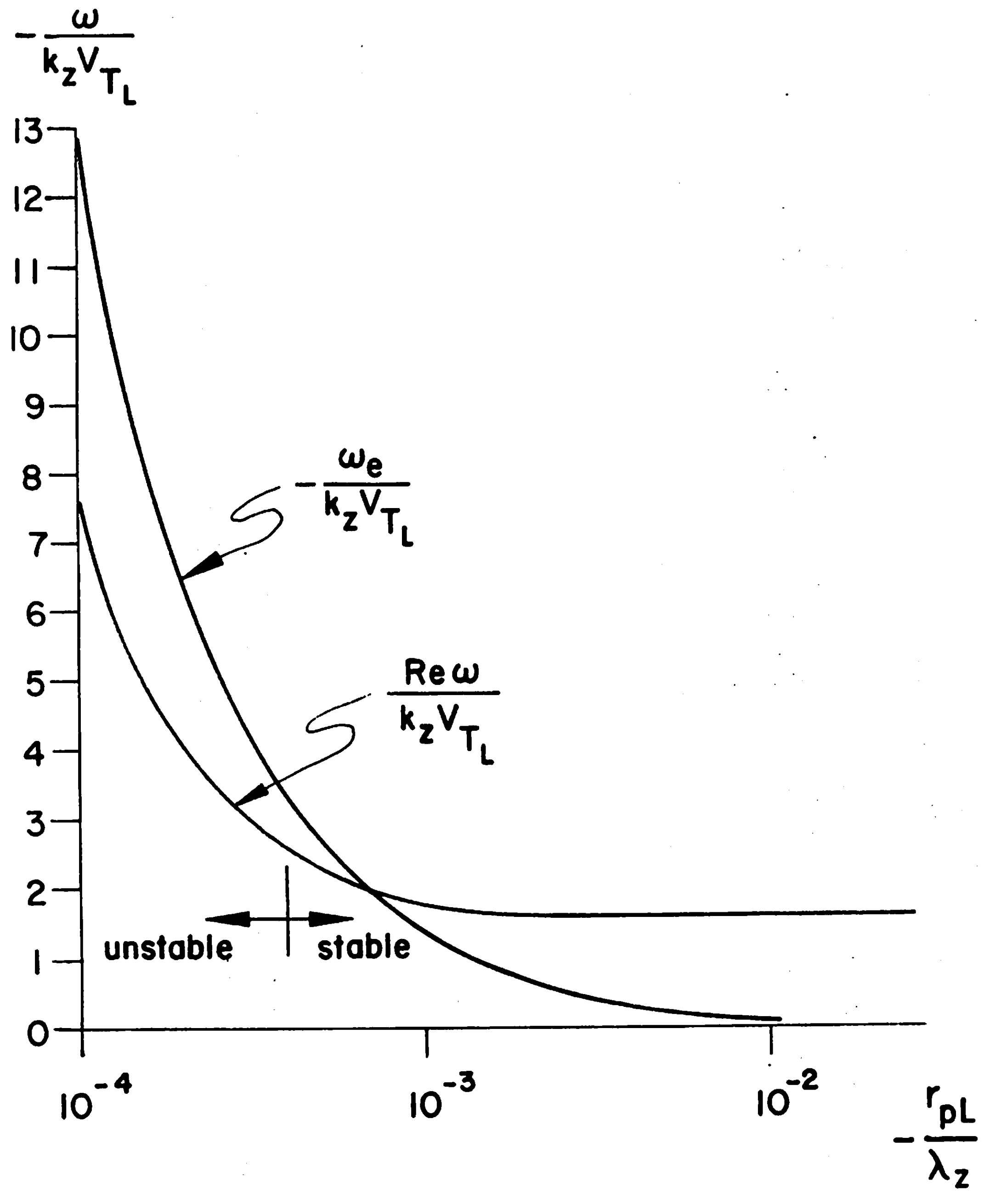

$\frac{\omega}{k_z V_{T_L}}$
13
12
11
10
9
8
7
6
5
4
3
2
1
0
$\frac{\omega_e}{k_z V_{T_L}}$
$\frac{Re\,\omega}{k_z V_{T_L}}$
unstable
stable
10^{-4}
10^{-3}
10^{-2}
$\frac{r_{pL}}{\lambda_z}$

Fig. 1c

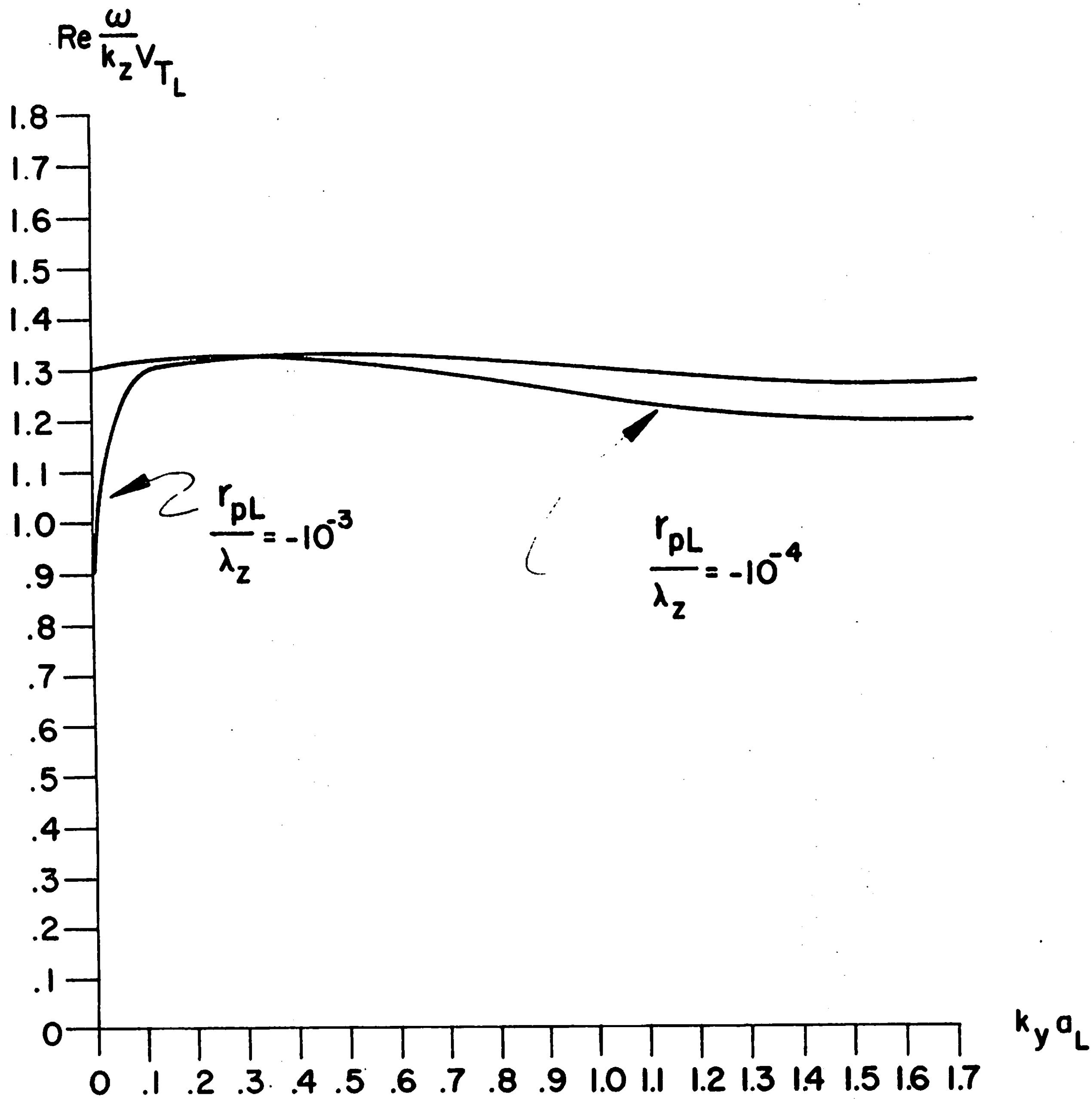

$\mathrm{Re}\,\frac{\omega}{k_z V_{T_L}}$
1.8
1.7
1.6
1.5
1.4
1.3
1.2
1.1
1.0
.9
.8
.7
.6
.5
.4
.3
.2
.1
0
$\frac{r_{pL}}{\lambda_z} = -10^{-3}$
$\frac{r_{pL}}{\lambda_z} = -10^{-4}$
0 .1 .2 .3 .4 .5 .6 .7 .8 .9 1.0 1.1 1.2 1.3 1.4 1.5 1.6 1.7
$k_y a_L$

Fig. 1d

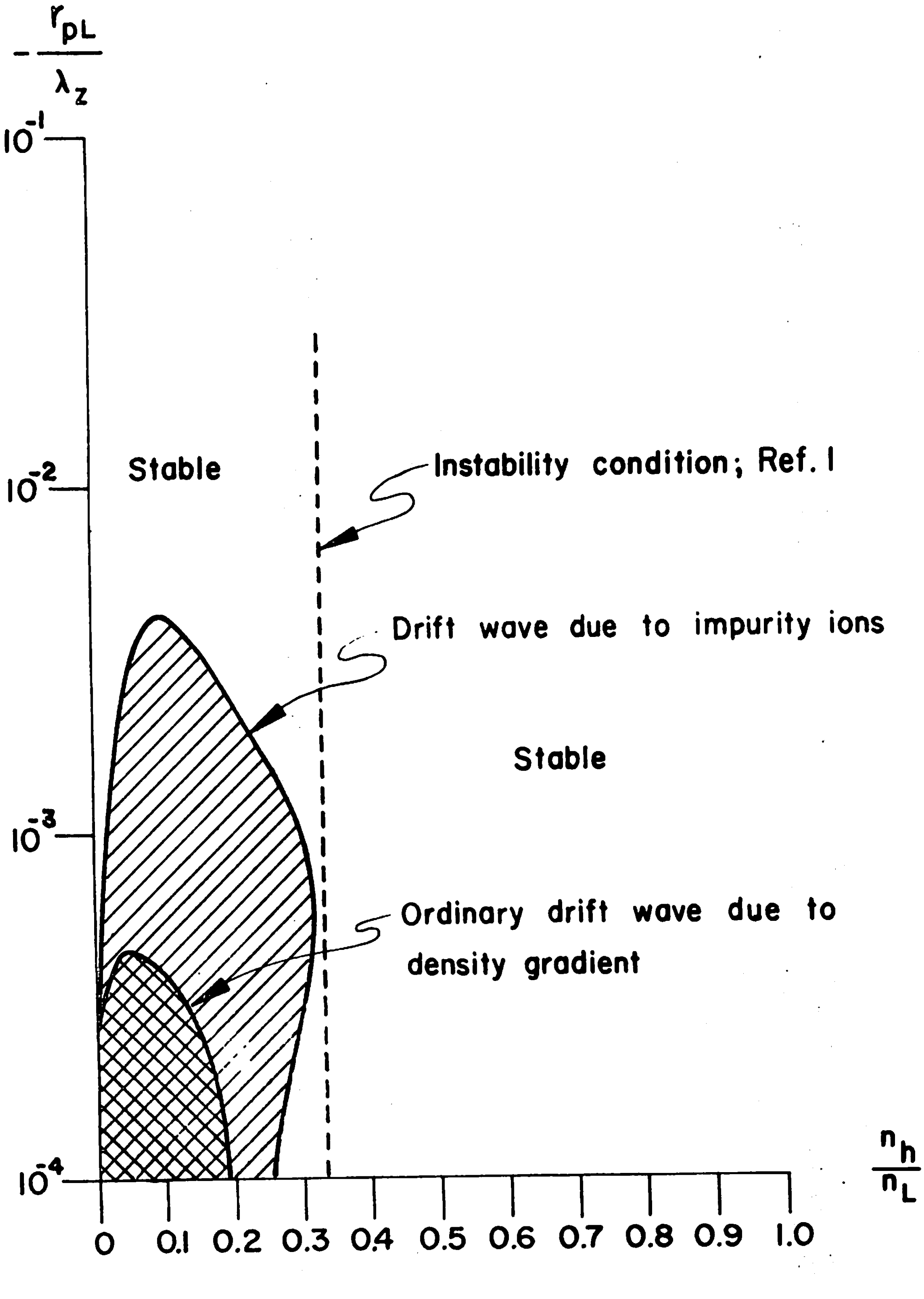
$-\frac{r_{pL}}{\lambda_z}$
10^{-1}
10^{-2}
10^{-3}
10^{-4}
Stable
Instability condition; Ref. 1
Drift wave due to impurity ions
Stable
Ordinary drift wave due to density gradient
$\frac{n_h}{n_L}$
0
0.1
0.2
0.3
0.4
0.5
0.6
0.7
0.8
0.9
1.0

Fig. 2

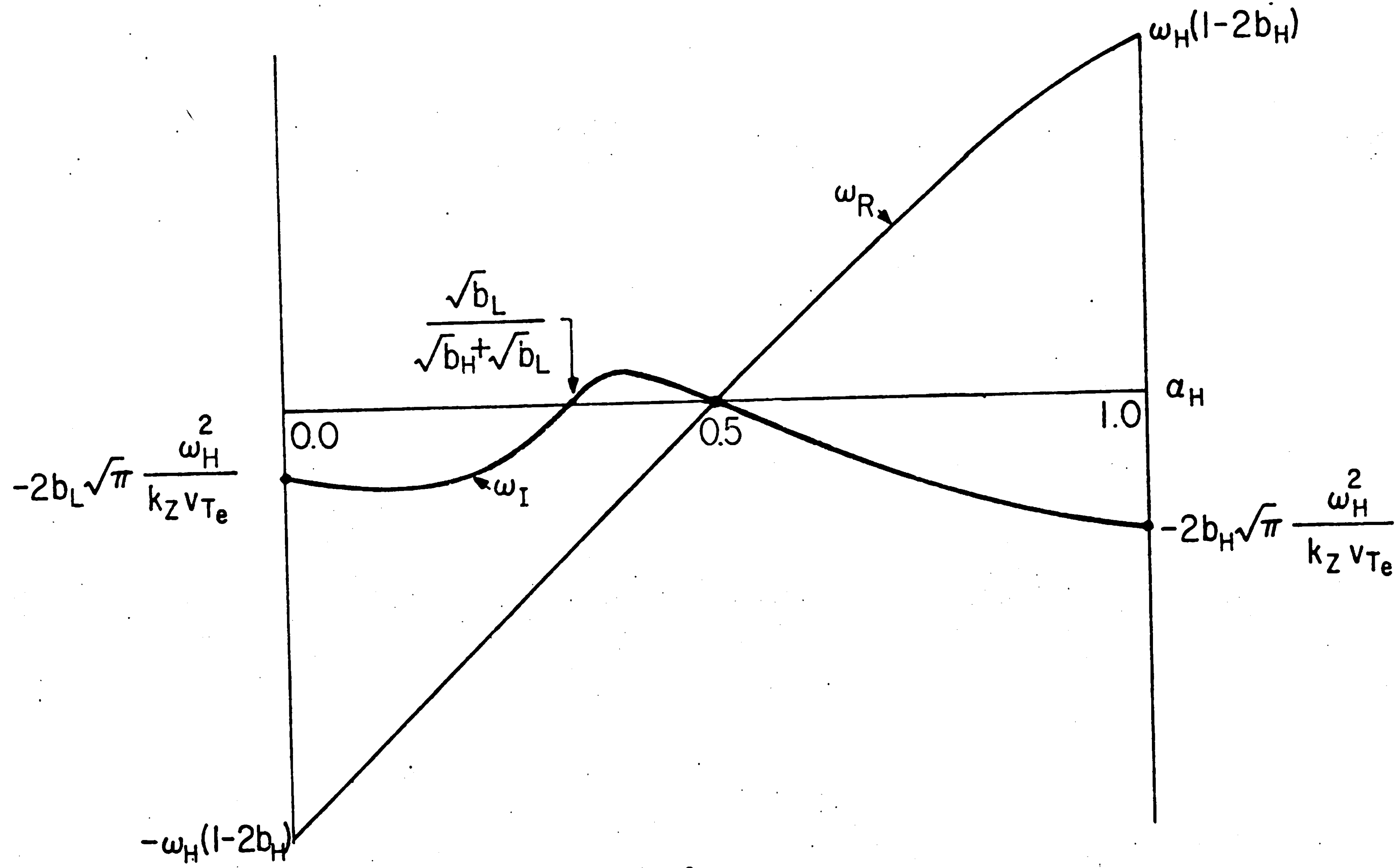

$\omega_H(1-2b_H)$
ω_R
$\frac{\sqrt{b_L}}{\sqrt{b_H}+\sqrt{b_L}}$
a_H
0.0
0.5
1.0
$-2b_L\sqrt{\pi}\,\frac{\omega_H^2}{k_z v_{T_e}}$
ω_I
$-2b_H\sqrt{\pi}\,\frac{\omega_H^2}{k_z v_{T_e}}$
$-\omega_H(1-2b_H)$

Fig. 3

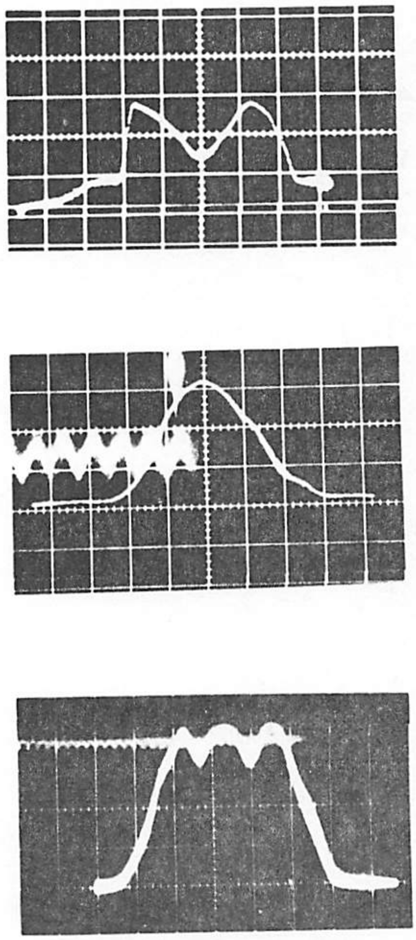

(a)

(b)

(c)

Fig. 4

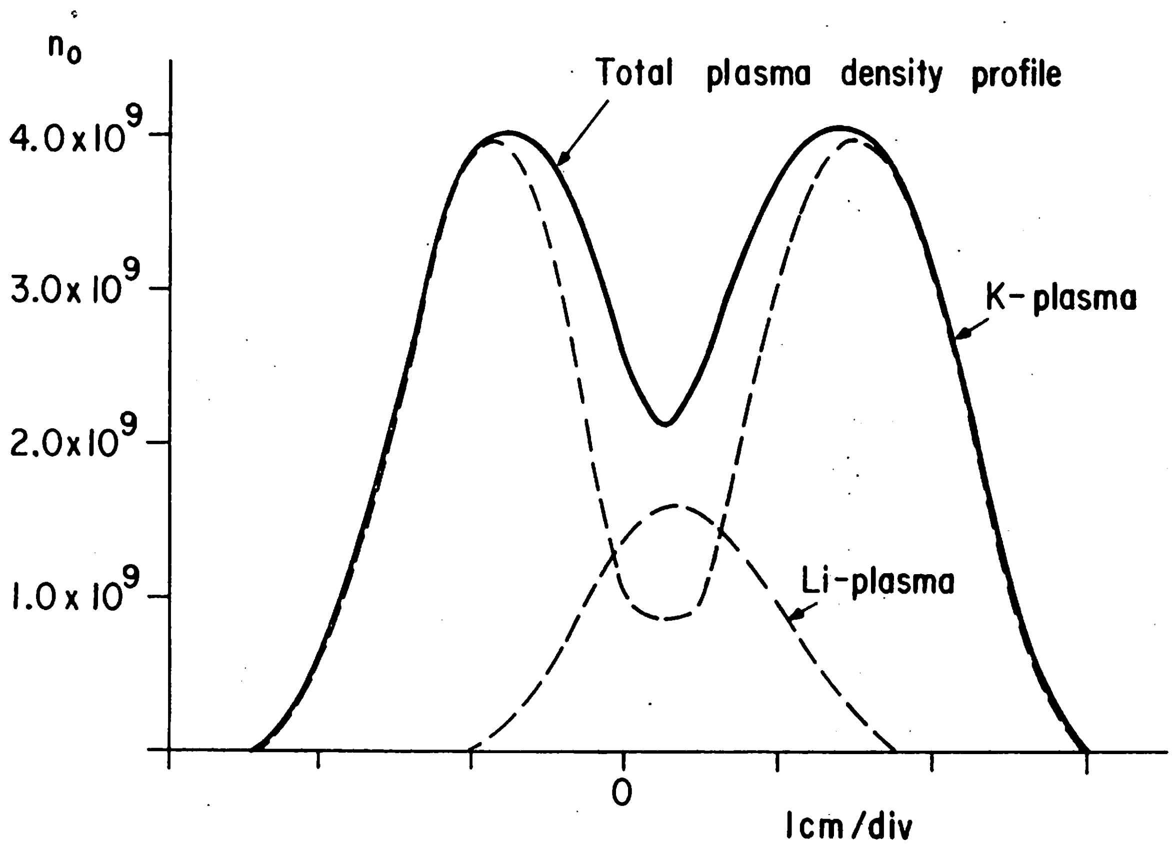

n_o
4.0×10^9
3.0×10^9
2.0×10^9
1.0×10^9
Total plasma density profile
K-plasma
Li-plasma
0
1cm/div

Fig. 4d